HardwareX (2018) e00036

Contents lists available at ScienceDirect

HardwareX

journal homepage: www.elsevier.com/locate/ohx

Hardware Article

Low-cost Sieverts-type apparatus for the study of hydriding/dehydriding reactions

Juan Luis Carrillo-Bucio [a], Juan Rogelio Tena-Garcia [a], Eduardo Paul Armenta-Garcia [a], Osiry Hernandez-Silva [b], José Gerardo Cabañas-Moreno [b], Karina Suárez-Alcántara [a,*]

[a] Unidad Morelia del Instituto de Investigaciones en Materiales de la Universidad Nacional Autónoma de México, Antigua Carretera a Pátzcuaro No. 8701, Col. Ex Hacienda de San José de la Huerta, C.P. 58190 Morelia, Michoacán, Mexico

[b] Programa de Nanociencias y Nanotecnología, Centro de Investigación y de Estudios Avanzados del IPN, Av. Instituto Politécnico Nacional No. 2508, Colonia San Pedro Zacatenco, CP 07360 Ciudad de México, Mexico

ARTICLE INFO

Article history:
Received 29 May 2018
Received in revised form 9 July 2018
Accepted 10 July 2018

Keywords:
Hydrogen storage
Sieverts-type apparatus
Hydriding/dehydriding reactions

ABSTRACT

The design and construction of a low-cost equipment for the study of hydriding/dehydriding reactions of different materials are presented. This is a Sieverts-type apparatus where a small amount (0.2–1 g) of solid hydrogen storage materials can be characterized. The apparatus combines the features of double lines (sample and reference) to eliminate small thermal effects on the reservoir and sample-holder volumes, with a $\Delta p = \Delta p_{sample} - \Delta p_{reference}$ approach to eliminate the need of a differential pressure transducer and to reduce costs. This apparatus can work from vacuum to 10 MPa hydrogen pressure and from room temperature to 673 K. Pressure, temperature and volume data are transformed by a real gases equation state and mass balance into hydrogen uptake or release in wt%. Characterization of typical hydrogen storage materials such as $LiAlH_4$ and Mg is presented to validate the performance of the apparatus.

Specifications Table

Hardware name	"Franky" Sieverts type apparatus
Subject area	Engineering and Material Science
Hardware type	Measuring physical properties and in-lab sensors
Open Source License	Creative Commons Attribution-ShareAlike license
Cost of Hardware	10,000 USD
Source File Repository	Open Science Framework: https://osf.io/zqvps/

* Corresponding author.
E-mail address: karina_suarez@iim.unam.mx (K. Suárez-Alcántara).

https://doi.org/10.1016/j.ohx.2018.e00036
2468-0672/

1. Hardware in context

Hydrogen storage technologies are emerging as basic and applied research topics in México. However, the number of research groups are very few as compared with other hydrogen technologies such as PEM-fuel cells or hydrogen production. One of the reasons for this is the high cost of specialized materials, safety systems, and apparatus for testing the hydrogen capture/release properties of solid materials. Thus, an important option is to develop low-cost apparatus for characterization of hydrogen storage materials. In our case, the apparatus must meet the particular conditions of temperature and pressures for the hydriding/dehydriding reactions of the materials studied at the Institute of Materials Research (Morelia): from room temperature to 673 K and from vacuum to 10 MPa hydrogen pressure.

In a general way, the sorption apparatus can be classified as gravimetric or manometric, according to the key variable to be controlled and recorded: mass (weight) or pressure. Each type of apparatus has advantages and disadvantages regarding the simplicity of construction, operation, maintenance, working principle, and cost [1–4]. Here, we present details of the construction of a manometric or Sieverts-type apparatus.

Some Sieverts-type apparatus for the study of hydrogen sorption/desorption reactions are composed of a reservoir volume, a pressure transducer and sample-holder volume (Fig. 1a). Most commercial apparatus use this general configuration [5,6]. In those apparatus, the key variable is the difference of pressure between the pressure registered at time t (instant) minus the initial pressure ($\Delta p = p_{instant} - p_{initial}$). In a second design (Fig. 1b), the apparatus can use a second branch or line, twin of the first one (sample and reference) [7,8]. There, the key variable is the differential pressure between the sample and the reference lines. In this last design, the inaccuracies produced by small thermal variations are reduced. However, this design needs a differential pressure transducer with particular specifications regarding the construction materials, pressure range and accuracy. This leads to the use of expensive differential transducers. In the present work, we expose a low-cost alternative for the construction of a double-line apparatus.

2. Hardware description

Fig. 1c presents the basic design of our Sieverts type apparatus. We combined the double-line (sample and reference) configuration to reduce thermal effects, with the use of twin direct pressure transducers to reduce costs. Here the key variable is the difference of pressure between the pressure at time t (instant) minus the initial pressure at both sample and reference lines. This translates as a delta of deltas for the pressure change, namely [9]:

$$\Delta p = \Delta p_{sample} - \Delta p_{reference} \tag{1}$$

where $\Delta p_{sample} = p_{instant\text{-}sample} - p_{initial\text{-}sample}$, and $\Delta p_{reference} = p_{instant\text{-}reference} - p_{initial\text{-}reference}$.

At the beginning of the experiment, both (sample and reference) initial pressures are equal. During the experiment, the pressure of the reference is essentially constant unless small thermal changes happened. Meanwhile, the increase or reduction in the registered pressure at the sample line beyond the thermal effects indicates the release or the uptake of hydrogen, i.e. the dehydriding or dehydriding reactions, respectively.

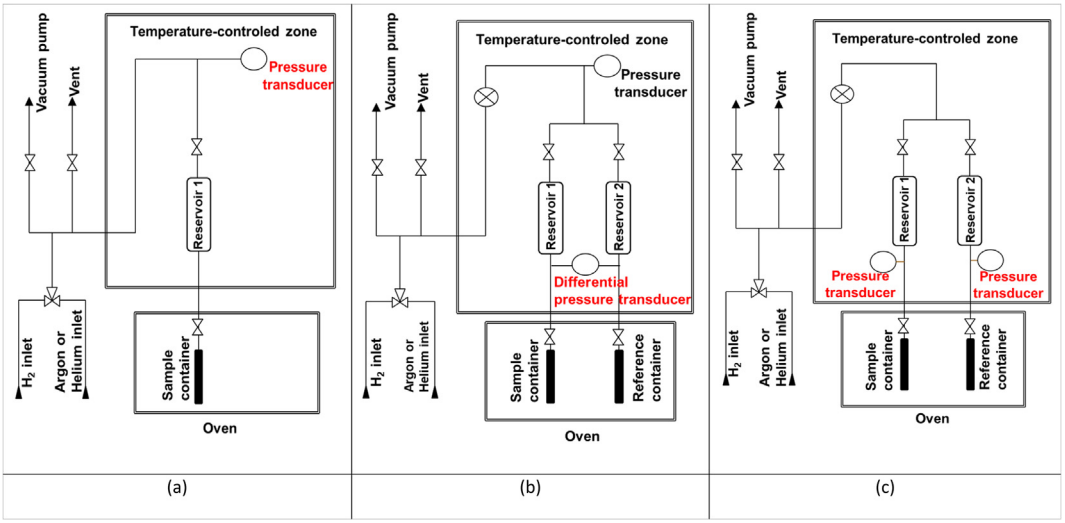

Fig. 1. Possible configurations of the manometric apparatus for the characterization of hydrogen hydriding/dehydriding reactions. (a) Single (sample) configuration. (b) Double (sample and reference) configuration with differential pressure transducers [8]. (c) Double (sample and reference) configuration with twin direct pressure transducers.

2.1. Transformation to hydrogen uptake/release in wt%

In the manometric apparatus, the measurements of H_2 pressure and temperature along with the knowledge of the void volume, an appropriate equation state for H_2 and a mass balance translate into hydrogen uptake/release in wt%. The calibration of this type of apparatus is performed to know the void volume at the sample holder and the reservoir [1–4,8]. In this work, we usually perform the calibration before the actual measurements with the use of argon. However, it also can be done after the hydriding/dehydriding reactions, depending on the sample stability. The volume of reservoir plus pipes of each line is 510 cm^3, and it is considered constant. Sample void volume is between 3 and 5 cm^3. The void volume within the sample-holder is less than 1% of the volume of the reservoir, thus the main contribution for the hydrogen uptake/release calculation is the reservoir volume. The quantity of sample normally used is 0.2–1 g, depending on the hydrogen storage capacity or content of each studied material.

The registered temperatures and pressures are converted to hydrogen uptake/release in wt% after the following formula [10]:

$$wt\%(H_2) = 100 * \frac{MH_2 * \Delta p * V_{sample}}{m * R * T_{sample} * Z_{fact}} + 100 * \frac{MH_2 * \Delta p * V_{reservoir}}{m * R * T_{reservoir} * Z_{fact}} \tag{2}$$

where MH_2 is the hydrogen molar mass (2.01588 g mol^{-1}). Δp is defined in Eq. (1). This Δp performs as a differential pressure transducer and helps reducing small (0.1 kPa) variations of the pressures caused by thermal effects. V and T are the void volume (in cm^3) and temperature (in Kelvin) of the reservoir and sample holder at the sample line. Due to void volumes are small we preferred to keep them in cm^3 and not in the SI unit, m^3. m is the sample mass in g; R is the gas constant, and Z_{fact} is the hydrogen compressibility factor [11,12]. The hydrogen compressibility factor can be calculated for a Hemmes real gas by using:

$$\left(p + \frac{a(p)}{V_m^{\alpha}}\right)(V_m - b(p)) = R * T \tag{3}$$

where b and a have a p (in bar) dependence:

$$a(p) = exp^{[19.599 - 0.8946 * \ln(p) - exp(-18.608 + 2.6013 * \ln(p))]} \quad (\text{for} p > 1 \quad bar) \tag{4}$$

$$b(p) = \left\{ \begin{array}{c} \sum_{i=0}^{8} b_i * ln(p)^i (p \geq 100 \ \ bar) \\ b(100)(p < 100 \ \ bar) \end{array} \right\} \tag{5}$$

where the b_i values are given in Table 1.

Meanwhile, α, the exponent of V_m in the first term of Eq. (3), has a T dependence. For T ≤ 300 K:

$$\alpha(T) = 2.9315 - 1.531 \times 10^{-3} * T + 4.154 \times 10^{-6} * T^2 \tag{6}$$

For T > 300 K, take $\alpha(300)$.

Pressures in Eq. (2) can be used in bar together with Eqs. (3)–(6). The formulae for the calculation of the compressibility factor originally were reported in bar and we recommend use it in bar [11,12]. In this case R = 83.14459 cm^3 bar K^{-1} mol^{-1}.

The calculation of Z_{fact} can be implemented as a macro in excel, python or other code, by using iterative root finders such as the *regula falsi*, Newton-Rapson, etc. [13]. The first step is to solve Eq. (3) for the molar volume using Eqs. (4), (5) and (6) for each measurement of p and T under an appropriate accuracy level for the reservoir and the sample holder. Then Z_{fact} for the reservoir and the sample holder can be obtained by using:

$$Z_{fact} = \frac{p * V_m}{R * T} Z = \frac{p * V_m}{R * T} \tag{7}$$

As an iterative method, the calculation of the compressibility factor can be time and effort consuming. As an alternative, a virial-type equation by Lemmon-Huber-Leachman [14] can be used:

$$Z = 1 + \sum_{i=1}^{9} a_i \left(\frac{100\text{K}}{T}\right)^{b_i} \left(\frac{p}{1MPa}\right)^{c_i} \tag{8}$$

Table 1
b_i values for Hemmes equation of state [11,12].

b_i	values	b_i	values
b_0	20.285	b_5	−0.12385414
b_1	−7.44171	b_6	9.8570583×10^{-3}
b_2	7.318565	b_7	$-4.1153723 \times 10^{-4}$
b_3	−3.463717	b_8	7.02499×10^{-6}
b_4	0.87372903		

Table 2
Coefficients for the Lemmon-Huber-Leachman equation [14].

i	a_1	b_i	c_i
1	0.05888460	1.325	1.0
2	−0.06136111	1.87	1.0
3	−0.002650473	2.5	2.0
4	0.002731125	2.8	2.0
5	0.001802374	2.938	2.42
6	−0.001150707	3.14	2.63
7	0.9588528×10^{-4}	3.37	3.0
8	$-0.1109040 \times 10^{-6}$	3.75	4.0
9	0.1264403×10^{-9}	4.0	5.0

where the temperature is in K and pressure is in MPa. Table 2 gives the coefficients for Eq. (8). We use and recommend this method due to the simplicity of the calculation and the good results observed. If this method is used, remember that R in Eq. (2) must be 8.314459 cm^3 MPa K^{-1} mol^{-1}.

The supplementary file ZETA contains some calculated values of Z for several equations of state. The selected values of pressure and temperature are in the range of operation of our Sieverts-type apparatus.

2.2. Mechanical design

The configuration of Fig. 1c was translated into the mechanical design (shown in Fig. 2a and supplementary files). The second part of the design work was the selection of the pieces for construction. Pipes, vessels, valves, and accessories were selected based on the temperature and pressure of operation; i.e. up to 10 MPa and 673.15 K. The selection included the application of Eq. (9) for vessels. The required thickness of vessels (reservoirs) were calculated following the ASME code [15]:

$$t = \frac{pR}{2SE + 0.4p} \tag{9}$$

where, p is the service pressure in psi (10 MPa = 1450.37 psi). R is the internal radius of the tank in inches: R = 0.9019 in (data from Swagelok®). S = 13200, and E = 0.45 [15]. From Eq. (9) a value of 1.93 mm thickness was required. The vessel thickness was selected as 2.24 mm. The selected brand for pipes, vessels, valves, and accessories was Swagelok®. All pieces were made of 316L stainless steel. All valves are manual.

2.3. Sample-holder design

The body of the sample holder is a simple design, quite common to other hydriding/dehydriding apparatus. The body of the sample holder (Fig. 2b) was machined in a single piece of 316L stainless steel and welded to Swagelok® VCR fittings. The

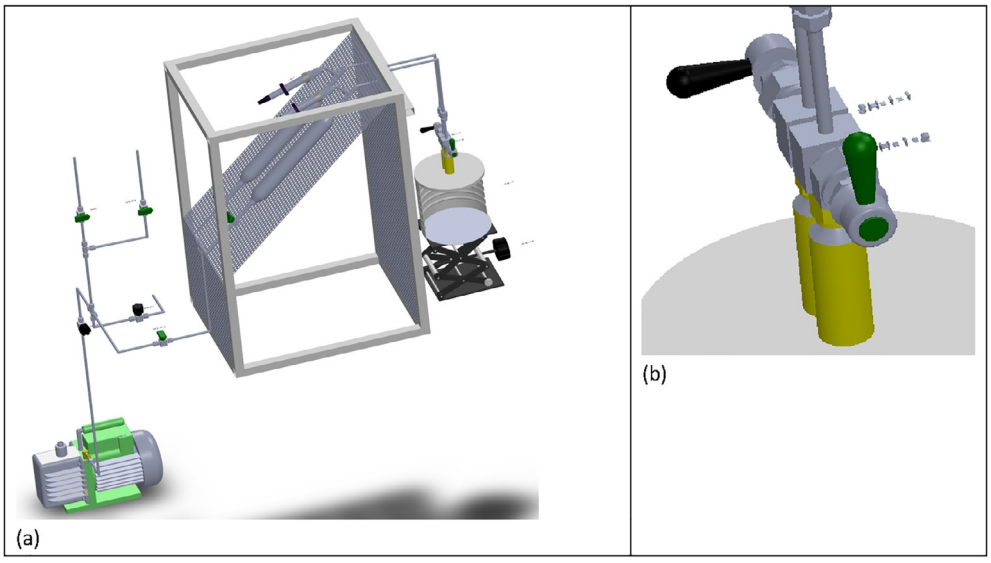

Fig. 2. (a) Mechanical design of the apparatus, and (b) design of the body of sample-holder.

wall thickness is 7.2 mm, thick enough to support the conditions of pressure and temperature. In our design, the sample holder is complemented with a diaphragm valve (Fig. 2a, piece SH-1) for protection of the samples against moisture and oxygen, and connected with VCR fittings to the apparatus. The volume of this accessory is considered in the reservoir volume since this piece is not inside the oven during experiments. The oven can be moved up and down to adjust its position for experiments.

2.4. Electrical design

All the electronic components work with an input AC of 120 V and 60 Hz. The most power-consuming part is the oven. It is composed essentially of a 480 W electric resistance. The second power-consuming part is the heater of the reservoirs. It is composed of two (twin) 100 W electric resistances connected to the same temperature controller. The rest of components are common solid state relays and electric breakers. The electric diagram is presented at Fig. 3.

2.5. Instrumentation

The instrumentation of the apparatus is: i) 2 highly-precise pressure transducers (10 MPa, 0.01% FS, series 33X, Keller), both transducers include temperature probes. ii) 3 high-precision controllers of temperature for the oven (sample and reference) and reservoirs (sample and reference). All temperature controllers are TK-series of Autonics. The temperature controllers and pressure transducers can collect data as quickly as one reading every millisecond. However, they are normally settled to take readings every 5 s. The temperature controllers and pressure transducers have a connection to a computer via USB (Tables 3 and 4).

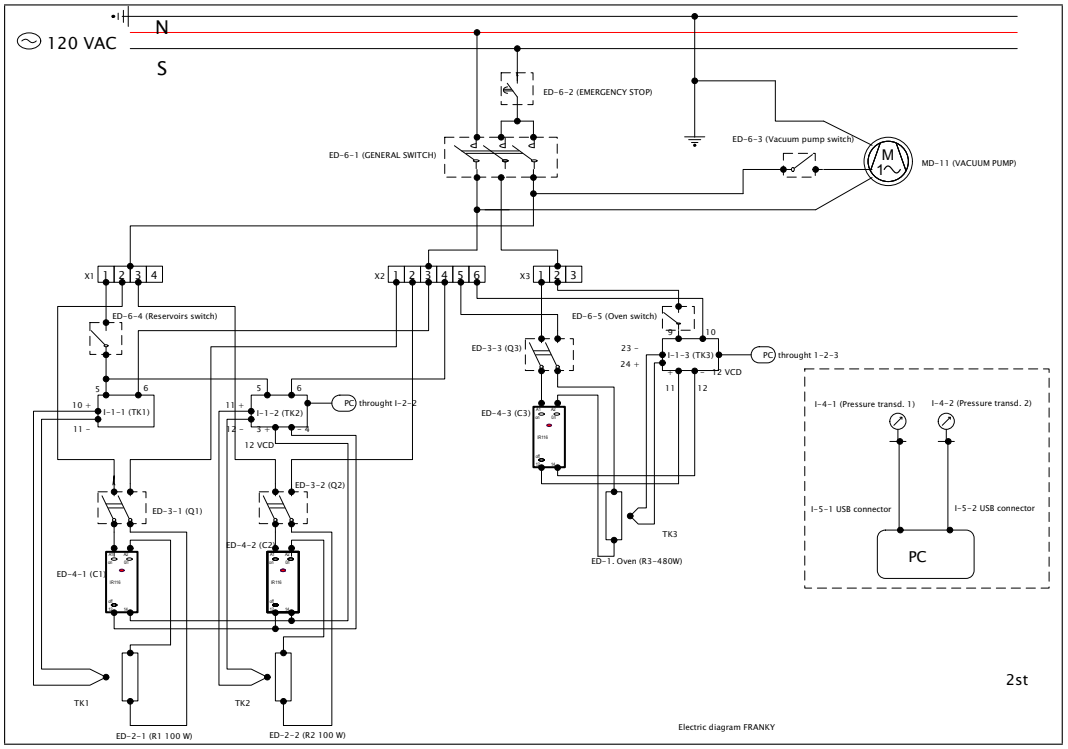

Fig. 3. Electric diagram of the apparatus.

Table 3
Design files summary.

Design file name	File type	Open source license	Location of the file
Mechanical design: machine	Solid works (Fig. 2a)	Attribution-Share Alike 4.0 International	https://osf.io/zqvps/
Electrical design: ELECTRICO 2da revision	ProfiCAD (Fig. 3)	Attribution-Share Alike 4.0 International	https://osf.io/zqvps/

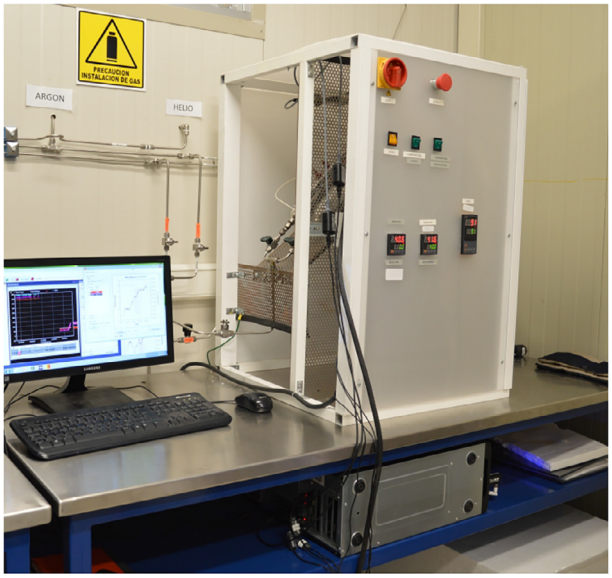

Fig. 4. The Sieverts-type apparatus designed and constructed at the Morelia-IIM of the UNAM, Mexico.

With these characteristics, our Sieverts-type apparatus can be used for the characterization of hydriding/dehydriding reactions in materials such as:

- Borohydrides, alanates, Mg-MgH_2, reactive hydride composites, etc.

Our Sieverts-type apparatus can perform:

- Temperature programmed adsorption (hydriding) experiments
- Temperature programmed desorption (dehydriding) experiments
- Hydriding/dehydriding experiments under isothermal conditions

Physically, the apparatus looked as shown in Fig. 4 before installing the thermal isolation and external plastic panels.

3. Design files

Mechanical design. This file contains the details about the mechanical design, including detailed piece numbering. *Electrical design.* This file contains the electric diagram, including detailed piece numbering.

4. Bill of materials

The design and construction of the apparatus lasted approximately 2.5 years. The purchases were performed in Mexican pesos (MXP), an average exchange of 18 MXP for 1 USD was considered (Table 4).

5. Build instructions

5.1. Mechanical construction: construction of the main structure of the apparatus

- Connect the MD-1 vessels to the MD-9 connectors to change from ¼ in NTP to ¼ in ISO finishes, at both ends of the vessels. At the lower end of each vessel, an MD-4 valve must be attached by means of a small pipe (2.5 cm) and ferrule-nut couples. The ferrules and nuts come with each accessory (valves, tee, cross, etc.). At the upper part of vessels connect an MD-5 tee by means of a small pipe (2.5 cm).
- The upper branch of each tee holds a 7 cm long pipe that is attached in turn to an MD-10 connector. This, in turn, must hold an I-4-pressure transducer.
- The remaining branch must connect to a 51 cm pipe welded to an MD-7 welding VCR fitting with its respective VCR nut (MD-8 VCR nut). This VCR fitting connects to the diaphragm valve of sample holder (SH-1 valves).

Table 4
Bill of materials.

Designator	Component	Number	Cost per unit-USD	Total cost-USD	Source of materials	Material type
Mechanical design (MD)	MD-1. Vessel for reservoirs	2 (MD-1-1 and MD-1-2)	210	420	Swagelok ® 316L-HDF4-500-PD	316L Stainless steel
	MD-2. Pipe	1 (various segments)	125	125	Swagelok ® SS-T4-S-035-20	316L Stainless steel
	MD-3. Needle valve	2 (MD-3-1 and MD-3-2)	225	450	Swagelok ® SS-14DKS4	316L Stainless steel
	MD-4. Valve	4 (MD-4-1, MD-4-2, MD-4-3 and MD-4-4)	450	1800	Swagelok ® SS-4P4T-M1	316L Stainless steel
	MD-5. Tee	3 (MD-5-1, MD-5-2, and MD-5-3)	26	78	Swagelok ® SS-400-3	316L Stainless steel
	MD-6. Cross union	1	25	25	Swagelok ® SS-400-4	316L Stainless steel
	MD-7. Welding VCR fittings	2 (MD-7-1 and MD-7-2)	8	16	Swagelok ® SS-8-CVR-3	316L Stainless steel
	MD-8. VCR Nut	2 (MD-8-1 and MD-8-2)	5	10	Swagelok ® SS-4-VCR-1	316L Stainless steel
	MD-9. Connector NPT	4 (MD-9-1, MD-9-2, MD-9-3 and MD-9-4)	20	80	Swagelok ® SS-400-1-4	316L Stainless steel
	MD-10. Connector	2 (MD-10-1 and MD-10-2)	30	60	Swagelok ® SS-400-7-6RJ	316L Stainless steel
	MD-11. Vacuum Pump	1	420	420	Yellow J 1/2HP 7CFM bullet. Serie: 156,789	316L Stainless steel
	MD-12. Aluminum box, thermal insulation and plastic for panels	1	100	100	Generic at local hardware store	Aluminum, glass fiber, acrylic.
	MD-13. Elevator	1	525	0 (donation)	Swiss Boy lab jacks. Aldrich Z635537	Aluminum
Sample-holder	SH-1. Diaphragm valve	2 (SH-1-1 and SH-1-2)	405	810	Swagelok ® SS-DLVCR4-PX	316L Stainless steel
	SH-2. VCR connector	2 (SH-2-1 and SH-2-2)	55	110	Swagelok ® SS-4-WVCR-6-400	316L Stainless steel
	SH-3. Body, machining and welding.	2 (SH-3-1 and SH-3-2)	27.5	55	Local distributor of metals.	316L Stainless steel
	SH-4. VCR filter	2 (each experiment)	10.5	21	Swagelok ® SS-4-VCR-2-2M	316L Stainless steel
Electrical design	ED-1. Oven	1	370	370	Glass-Col Heating Mantle. Aldrich Z505897-1EA	Aluminum
	ED-2. Heaters (100 W resistances (R1 and R2))	2 (ED-2-1 and ED-2-2)	27.5	55	Band resistance. Local engineering service.	Aluminum
	ED-3. Breakers	3 (ED-3-1, ED-3-2 and ED-3-3)	20	60	Eaton 20 A. Local electronic store.	Metal/plastic
	ED-4. Solid state relays	3 (ED-4-1, ED-4-2 and ED-4-3)	50	150	Siemens 20 A. Local electronic store	Metal/plastic
	ED-5. Cable	3 (meters)	2	6	Local electronic store	Metal/plastic
	ED-6. Switches	5 (various models) ((ED-6-1, ED-6-2, ED-6-3, ED-6-4, ED-6-5 and ED-6-6)	1	5	Local electronic store	Metal/plastic
Instrumentation	I-1. Temperature controller PID	3 (I-1-1, I-1-2 and I-1-3)	100	300	TK4-serie. Autonics.	Metal/plastic
	I-2. USB connector of temperature controller	3 (I-2-1, I-2-2 and I-2-3)	111	333	USB Cable. Autonics	Metal/plastic
	I-3. Thermocouple J	3 (I-3-1, I-3-2 and I-3-3)	31	93	Local engineering service/calibration.	Metal
	I-4. Pressure transducer	2 (I-4-1 and I-4-2)	1515	3030	KELLER PA-33X/0-100 bar/RS485 4-20 mA/ 0,01%FS	316L Stainless steel
	I-5. USB connector of Pressure transducer	2 (I-5-1 and I-5-2)	230	460	KELLER K114-B	Metal/plastic
	PC	1	500	500	DELL-PC	Metal/plastic

- The reservoir volume of each line (sample and reference) is defined from the MD-4 valve up to the diaphragm valve of the sample-holder, including the branch that connects the pressure transducer. The relevant volume for calculations, i.e., the vessel volume plus that of pipes and accessories was measured with pure water and compared to a calculation based on the manufacturer specifications. This volume is considered constant, namely, 510 cm^3.
- At the bottom of the arrangement, the two twin vessels are connected to an MD-5 tee by means of a 10 cm pipe. The pipe is folded 90°. The third branch of this MD-5 Tee is connected to the main inlet valve (MD-4-3).

- This, in turn, is connected to the MD-6 cross union to distribute pipes for vacuum, vent, argon inlet and hydrogen lines. The hydrogen and argon inlets have MD-5 valves. On the other hand, the vacuum and argon lines have MD-3 needle valves for better control of outlet flows. The longitude and space distribution of pipes connecting these pieces are free, since that this volume is not used for calculations.
- Before operation, all joints were tested for leaks. Once in operation, the joints are periodically tested for leaks.
- The mechanical components were fixed inside of an aluminum box. The aluminum box was divided into two compartments. One at the back for the mechanical components (83 cm $\times$ 55 cm $\times$ 40 cm) and one at the front for electrical components (83 cm $\times$ 55 cm $\times$ 20 cm).

5.2. Sample-holder construction

- The construction of the sample holder is relatively easy. First, a hole was drilled in a 316L stainless steel cold-rolled piece (SH-3), its dimensions are indicated at the corresponding diagram-file. Then, this piece was welded to a VCR connector (SH-2) to form the body of the sample holder. The volume of the body of the sample-holder is 6.6 cm^3. This piece must comply with the norms for pressure vessels and the welding must be inspected before use. Finally, this piece is connected to a diaphragm valve (SH-1). Between the body of the sample holder and the valve, an SH-4 VCR filter is placed. In turn, the whole sample holder is attached to the apparatus by the upper end of the diaphragm valve (SH-1), using another SH-4 VCR filter. The two filters are replaced every time a different sample is tested.

5.3. Assembly of the electrical components

- The electrical connections must follow the diagram in Fig. 3. Essentially the apparatus is composed of the main switch, an emergency stop, oven, reservoir heaters, and vacuum pump switches. The oven, heaters, and vacuum pump have an individual manual switch. For the oven and reservoir heaters, the switches are connected to the breakers, then to solid state relays, and finally to the resistances. The reservoirs heaters are both connected to the I-1-2 temperature controller. Meanwhile the I-1-1 temperature controller is just sensing. The configuration can be quickly changed to both temperature controllers controlling.

5.4. Instrumentation

- The temperature controllers (I-1-1, I-1-2, and I-1-3) are powered as indicated by the electrical diagram. All of them need a temperature probe; our selection for this was 3 thermocouples type J (I-3-1, I-3-2 and I-3-3). The temperature controllers are run (programming of test temperature, heating rate, etc.) by means of a PC and a USB connector (I-2-1, I-2-2, and I-2-3). The software is DAQmaster of Autonics. It is recommended to read the user manual of this software.
- The pressure transducers (I-4-1 and I-4-2) are powered by the PC through USB connector (I-5-1 and I-5-2). Data are collected by means of the Control Center Series 30 software of Keller. It is recommended to read the user manual of this software.
- Temperature and pressure instruments work fine regarding the quantity of data collected and frequency/speed of data collection. However, from our particular experience temperature controllers of Autonics frequently have connection problems at the time of setting-up the experiments, i. e., at the time of first connection.

6. Operation instructions

Below we describe the operation instructions. The pressure are given in absolute values in kPa or MPa and Kelvin for temperature. Unless otherwise indicated, the volume values are expressed in cm^3.

a) System preparation. Weigh the sample. The recommended weight of the sample is between 0.2 and 1 g. For example, for a Mg sample, about 0.7–1 g is recommended. Place the sample in the body of the sample holder. The sample holder must be neatly clean. Attach the sample-holder body to the diaphragm valve, tighten properly. All these operations must be performed in an argon-filled glove-box if the materials are oxygen and moisture sensitive. Close the valve and transfer to the apparatus, tighten properly to ensure no leaks. The sample holder at the reference side is normally kept in place.
b) Power on the apparatus and PC. Open the DAQmaster and Keller software for temperature and pressure records, respectively. From this point, the pressures and temperatures must be recorded at all time. A good recording rate is a set of readings of pressures and temperatures every 5 sec. In the current state of the apparatus, the collected data is processed first by the Keller and Autonics software and then exported manually to an excel datasheet. A further improvement would include data processing by using specialized software such as LabVIEW or equivalent.
c) Warm up the reservoirs to any temperature above ambient temperature, a value between 293.15 and 318.15 K is recommended. Warm up the oven at the same temperature. At our lab, the ambient temperature is constant at 291.15 K, thus an apparatus temperature between 296.15 and 298.15 K is frequently used.

d) Evacuate the air in the apparatus by three successive cycles of vacuum and argon inlet at 0.2–0.6 MPa (0.6 MPa is recommended). The diaphragm valve that connects the apparatus and the sample-holder at the sample side must be closed during the procedure. The diaphragm valve that connects the apparatus and the sample-holder at the reference side must remain open during the procedure. Close the main valve (MD-4-3) at the end of the procedure leaving the apparatus full of argon (0.6 MPa).

e) Calibration of void volume. Once the pressure and temperature are stable, record manually (log book) these values. Open the diaphragm valve that connects the apparatus and the sample-holder at the sample side. Record manually (log book) the new values of pressure and temperature. Alternatively, you can record the exact time before and after expansion, and later read the data from the DAQmaster and Keller files. Apply the following formula to estimate the void volume at the sample holder:

$$\frac{p_1 * V_1}{R * T_1} = \frac{p_2 * V_2}{R * T_2} \tag{10}$$

f) p_1 and p_2 are the pressures before and after the opening of the diaphragm valve (expansion). T_1 is the temperature before expansion, T_2 is the temperature after the expansion (usually the change is very small). R is the ideal gas constant. $V_2 = V_1 + V_{sample}$, where V_2 is the total void volume, V_1 is the reservoir void volume (vessel, pipes and accessories, it is taken constant as 510 cm^3) and V_{sample} is the void volume of the sample holder (the same as in Eq. (2)). Solve for V_{sample}. This value is considered very important for further calculations. However, based on the data analysis and experience, the reservoir volume has more influence on the calculation of hydrogen released/stored (Eq. (2)). This occurs when the reservoir volume is big compared with the sample-holder void volume. Thus the void volume at the sample holder accounts approximately for less than 1% of the calculation.

g) The calculation of the void volume assumes that there is no argon sorption by the material and that the argon behaves as an ideal gas. This means that i) the number of argon moles is identical before and after the expansion ($n_1 = n_2$), and that ii) the relationship of Eq. (10) can be used.

h) Alternatively, one can pressurize the whole reservoir plus sample holder (higher than 0.6 MPa). Then, close the diaphragm valve and release the gas at the reservoir down to a very low value (for example to equal the atmospheric pressure, 81.3 kPa (absolute pressure at Morelia City)). This leaves the sample holder under pressure and the reservoir volume at low pressure. Once at thermal equilibrium, open the diaphragm valve, register the change of pressure and apply Eq. (10).

i) Open all valves and evacuate the argon until vacuum is reached in all the apparatus, including sample-holders. For example, in vacuum, an absolute pressure of 0.2 kPa can be reached by our vacuum pump (MD-11 part).

j) Temperature programmed desorption or sorption. Set the initial working pressure. It is large for hydriding reactions (normally between 2.5 and 5.0 MPa for our materials). It is low for dehydriding reactions (0–0.5 MPa for our materials). Close all valves but the diaphragm valve that connects the apparatus and the sample holder at both lines (sample and reference).

k) Set the target temperature and the heating rate. In our experiments, heating rates of 1, 5 or 10 K/min are frequently used. The Autonics program will reach the test temperature and then keep it constant until further instructions.

l) Let the system react to the desired level.

m) After the reaction, let the system cool down to room temperature. With the Autonics software one can program a cooling rate or just let cooling occur.

n) Release the remaining pressure, then fill the apparatus with argon at low pressure.

o) Close the diaphragm valve that connects the apparatus with the sample holder. Free the sample holder, transfer it to the glove box and recover the sample for further characterization.

p) Isothermal experiments. For isothermal experiments follow the same procedure until step (i). Then set an adequate pressure for "protecting" the material during heating. For hydrogenation experiments, choose a pressure below the equilibrium pressure at the temperature of test or low enough to avoid hydrogenation. For dehydrogenation experiments, choose a pressure above the equilibrium pressure at the temperature of test or high enough to avoid dehydrogenation. Close the diaphragm valves.

q) Set the test temperature and the heating rate. In our experiments heating rates of 1, 5 or 10 K/min are frequently used. The Autonics program will reach the target temperature and then keep it constant until further instructions.

r) Once at the temperature for hydrogenation, set the pressure slightly above to the experiment pressure at reservoirs. This can lead to small temperature disturbances at the reservoir, allow for stabilization. Once the temperature has stabilized, open both diaphragm valves at the same time. This is the time zero of reaction.

s) For dehydrogenation, set the pressure slightly below the experiment pressure at reservoirs. This can lead to small temperature disturbances at the reservoir, allow for stabilization. Once the temperature has stabilized, open both diaphragm valves at the same time. This is the time zero of reaction.

t) To complete the cycling repeat steps (r) and (s) as many times as needed.

u) Data treatment. Alike the manual operation, data treatment is also a manual procedure, for now. We use an excel datasheet to calculate the hydrogen uptake/release (Fig. 5). First, the raw data of the DAQmaster and Keller software for

	A	B	C	D	E	F	G	H	I	J	K	L	M
1	time	t sample	t res	p sample	del P sample	p refencia	del P referenc	delta delta	Z sample	Z reservoir	wt sample	wt reservoir	wt% tota
2		ºC											
3													
4													
5	0	23	22	1.0295448	0	1.0326023	0	0	1.0005903	1.00059057	0.000000000000	0.000000000000	0.000000000000
6	0.00138889	23	22	1.0298901	0.0003453	1.0331268	0.0005245	-0.0001792	1.0005905	1.00059077	0.000007182880	0.000936478826	0.000943661706
7	0.00277778	23	22	1.0297279	0.0001831	1.0330276	0.0004253	-0.0002422	1.0005904	1.00059067	0.000009708112	0.001265709782	0.001275417894
8	0.00416667	23	22	1.0297718	0.000227	1.0327415	0.0001392	8.78E-05	1.00059043	1.0005907	-0.000003519291	-0.000458832849	-0.000462352140
9	0.00555556	23	22	1.02911	-0.0004348	1.0333309	0.0007286	-0.0011634	1.00059005	1.00059032	0.000046632625	0.006079798876	0.006126431501
10	0.00694444	23	22	1.0298996	0.0003548	1.0329056	0.0003033	5.15E-05	1.0005905	1.00059077	-0.000002064276	-0.000269133143	-0.000271197420

Fig. 5. Example of calculation of quantity of hydrogen uptake.

temperature and pressure must be exported to an Excel readable format. Then, the initial point (zero-time) of the experiment must be recognized. We normally select the zero-time of reaction as the time of the beginning of heating for temperature programmed adsorption and temperature programmed desorption experiments. For hydriding/dehydriding experiments under isothermal conditions, the zero is the time of opening of the diaphragm valves. Then copy the data to the datasheet and apply Eqs. (1), (2) and (8) to obtain the hydrogen uptake or release. Remember to update the value of the mass of sample, the calibrated void volume, and to include a proper exchange of K instead of °Celsius for temperature.

7. Validation and characterization

7.1. Temperature programed desorption (TPD)/$LiAlH_4$ material

The TPD method is used to investigate the events that take place in a material while its temperature is changed in a controlled manner [16]. TPD is quite common in the area of hydrogen storage. Thus, our apparatus should perform this type of experiments. $LiAlH_4$ is a well-known hydrogen storage material due to its facile dehydrogenation but almost impossible complete re-hydrogenation. Pure (and not milled) $LiAlH_4$ undergoes a phase transition at 433.15–450.15 K before undergoing a first dehydrogenation reaction to give Li_3AlH_6 and Al at 460.15–491.15 K (Eq. (11)). A second dehydrogenation reaction was observed to occur at 501.15–555.15 K to give LiH and Al (Eq. (12)) [17,18]:

$$LiAlH_4 \rightarrow 1/3\ Li_3AlH_6 + 2/3\ Al + H_2 \tag{11}$$

$$1/3\ Li_3AlH_6 \rightarrow LiH + 1/3Al + 1/2\ H_2 \tag{12}$$

Together, both reactions provide for a hydrogen release of 7.9 wt%. Additionally, ball milling [19] and the use of accelerators for the dehydrogenation reaction can reduce the dehydrogenation temperature. In our case, cryogenic milling was used to preserve the delicate $LiAlH_4$ during milling. Still more, in our research group, the cryo-milling has been particularly effective to improve hydrogen storage properties. The results of the dehydrogenation of cryo-ball milled $LiAlH_4$ are presented in Fig. 6. Frame (a) presents the foundation of this work: the use of a delta of deltas for the pressure (Eq. (1)). The subtraction of $\Delta P_{reference}$ from the ΔP_{sample} and the application of Eq. (2) leads to the curve of Fig. 6b, where the two reaction steps (Eqs. (11) and (12)) can be observed. The temperature at the middle of the first dehydrogenation wave (peak at the first derivative plot of the inset in frame b) is 427 K. Meanwhile, the second dehydrogenation peak temperature is located at 461 K. However, reporting the onset temperatures is more common. The onset temperatures are located roughly 15 K before the peak temperatures. The total quantity of released hydrogen was 7.5 wt%.

X-ray Diffraction (XRD) (Fig. 6c) and Fourier Transformed Infrared Spectroscopy (FT-IR) (Fig. 6d) confirm the occurrence of the dehydrogenation reaction. All the peaks of the blue-line diffractogram of the frame (c) corresponds to $LiAlH_4$ (ICSD-191838) [20]. The orange line presents the diffractogram of the dehydrogenated material, where the peaks correspond to the mixture of Al and LiH (ICSD-60600 and ICSD-61749). They present very similar crystal-cell size and the same symmetry space group, thus only a set of diffraction peaks are observed. The shape of the background and two peaks at roughly 22° and 26° are the Kapton contribution. In turn, frame (d) presents the FT-IR response. The $[AlH_4]^-$ ion presents two internal active modes in the infrared: the Al-H bending mode (600–1100 cm^{-1}) and the Al-H stretching mode (1600–2000 cm^{-1}) [20]. The cryo-ball milled $LiAlH_4$ presented both peaks, while at the dehydrogenated material only marginal (residual) response was obtained.

In general, TPD experiments are relatively easy to perform. Thus the first results of our apparatus were TPD experiments on $2LiBH_4$ + Al/additive [9].

7.2. Temperature programed sorption (TPS)/Mg material

Similar to TPD, following a sorption or hydrogenation reaction by means of controlled heating during exposition to medium-high hydrogen pressures is highly desirable. Some high-pressure calorimeters can perform this type of experiments. Our apparatus should also perform this type of experiments.

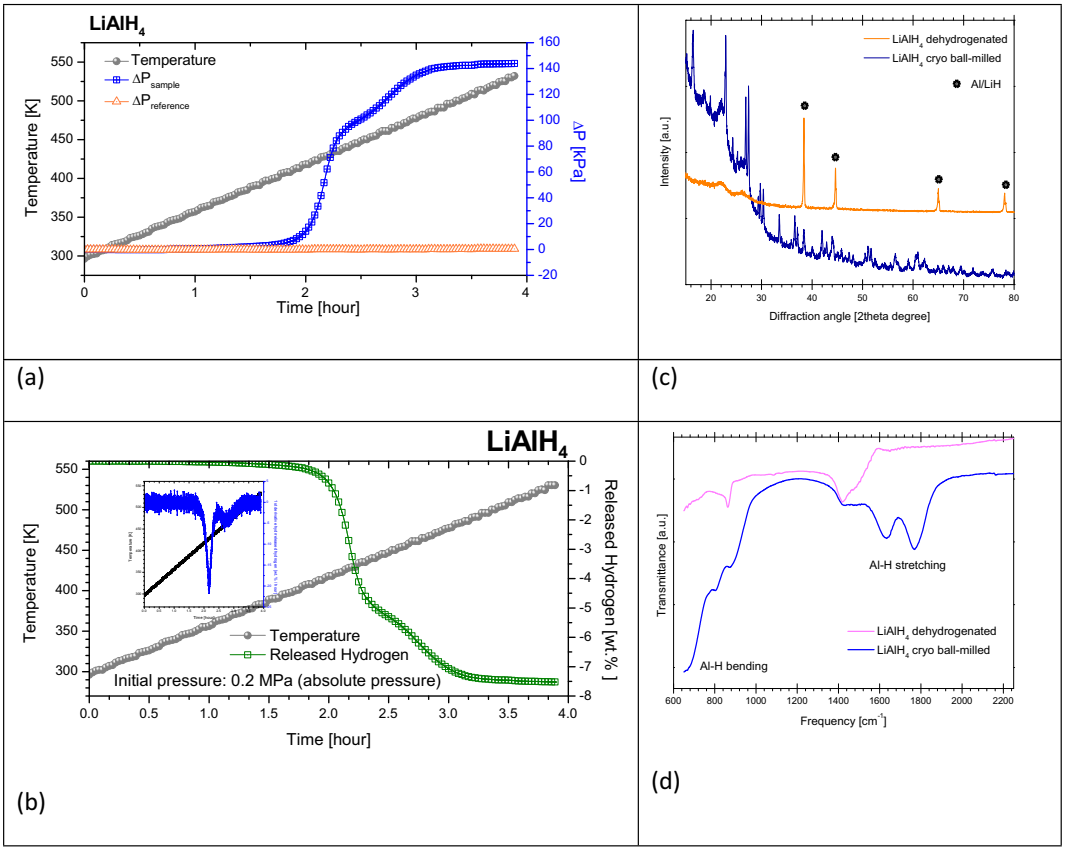

Fig. 6. Temperature programed desorption of $LiAlH_4$. (a) Foundations of this work, i.e. the use of Δp for describing the changes in the sample and reference pipelines or branches upon reactions. (b) Result of the dehydrogenation reaction performed as TPD. Inset: First derivative of the released hydrogen versus time, indicating the peak temperatures of the dehydrogenation steps. (c) and (d) XRD and FT-IR, respectively, before and after dehydrogenation for confirmation of reaction.

Mg is the most commonly studied hydrogen storage material, due to its relatively low-cost, easy conditioning (ball-milling) for hydrogen storage purposes and reversibility. Fig. 7a presents the first 3 hydrogenation reactions of Mg, limited to a time-window of 4 h. In between each of them, dehydrogenation was performed in dynamic vacuum. The first hydrogenation reached 2.3 wt%; the second 4.8 wt% and the third 5.1 wt%. The values are consistent with a progressive activation of the material. They are in the range of other Mg-materials produced by the same research group [21]. Small variations of the measured hydrogen uptake are due to the low quantity of sample used for this particular experiment. Larger samples usually lead to the reduction of these variations. The XRD of the milled and hydrogenated materials corroborate the partial hydrogenation of Mg after the 3rd hydrogenation. The diffraction pattern of hydrogenated Mg is composed of MgH_2, non-reacted Mg, and MgO. The MgO is commonly observed after heating Mg samples due to the crystallization of surface oxides [21].

7.3. Isothermal cycling experiments

The addition of some materials can lead to an improvement of the hydrogenation/dehydrogenation kinetics or the reduction of on-set temperatures. That is the case of the addition of nano/micro particles of Ni and C-nanotubes to a Mg matrix [22]. Nonetheless, sometimes these materials need a longer process of activation. Frames (a) and (b) of Fig. 8 present the activation cycle, with heating ramp, of a sample of Mg-Ni-C-nanotubes. The activation procedure consisted in the exposition to 2.6 MPa hydrogen pressure (absolute) and heating up to 648.15 K for several hours. Then, the sample was dehydrogenated at 0.1 MPa (absolute) and 623.15 K, also with heating ramp of 10 K/min.

After the activation, the material was kept at 623.15 K and two hydrogenation/dehydrogenation cycles were performed by alternating a hydrogen pressure of 1.6 MPa and 0.1 MPa (absolute), respectively. Fig. 8(c) and (d) present these cycles. These cycling experiments were restrained to 1.5 h under hydrogenation conditions and 1.5 h under dehydrogenations conditions. A progressive reduction of the time of reactions, particularly during hydrogenation, was observed. However, the first isothermal dehydrogenation was not complete after 1.5 h, thus it was forced by applying dynamic vacuum for 15 min.

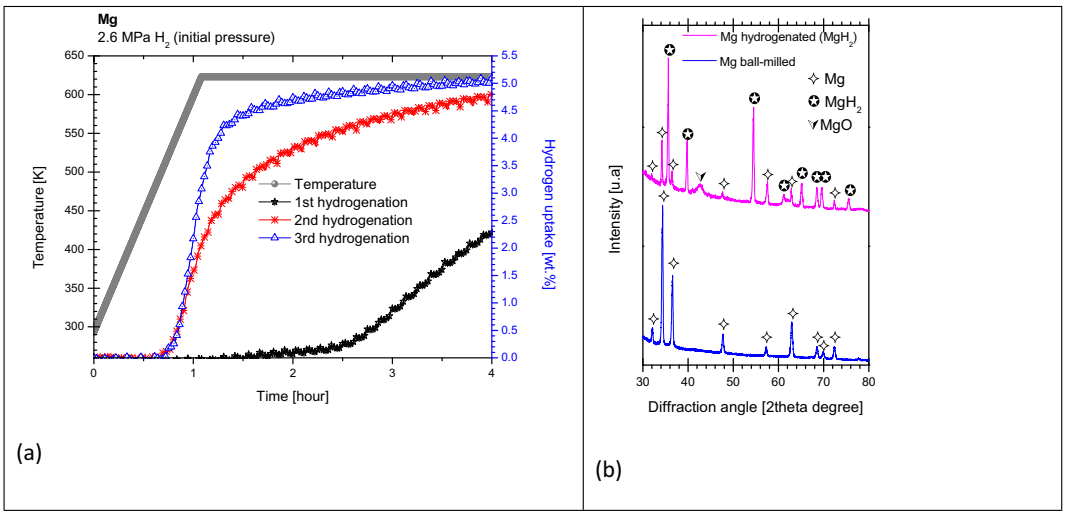

Fig. 7. Successive hydrogenation reactions on Mg. (a) Activation of the material upon successive hydrogenations. (b) XRD as milled and after hydrogenations for confirmation of reaction.

Despite of that, we can consider that the hydrogenation and dehydrogenation reactions are reversible in terms of the quantity of hydrogen stored/release. Also, the reaction is quicker than the reaction of Mg materials without additives.

7.4. Sample preparation and characterization

Well-known materials and some new materials for hydrogen storage were prepared and tested for hydrogenation/dehydrogenation in our apparatus. Below we present the details of the sample preparation and testing. Additionally, the materials were characterized before and after the hydrogenation or dehydrogenation reactions by means of XRD or FT-IR. XRD characterization was performed in a D2phaser diffractometer (CuK_α = 1.540598 Å). The powders were compacted in a dedicated sample-holder, and then they were covered with a Kapton foil for protection against ambient oxygen and moisture. Data processing and phase identification were performed with Diffract Suite Eva and MAUD software. ICSD

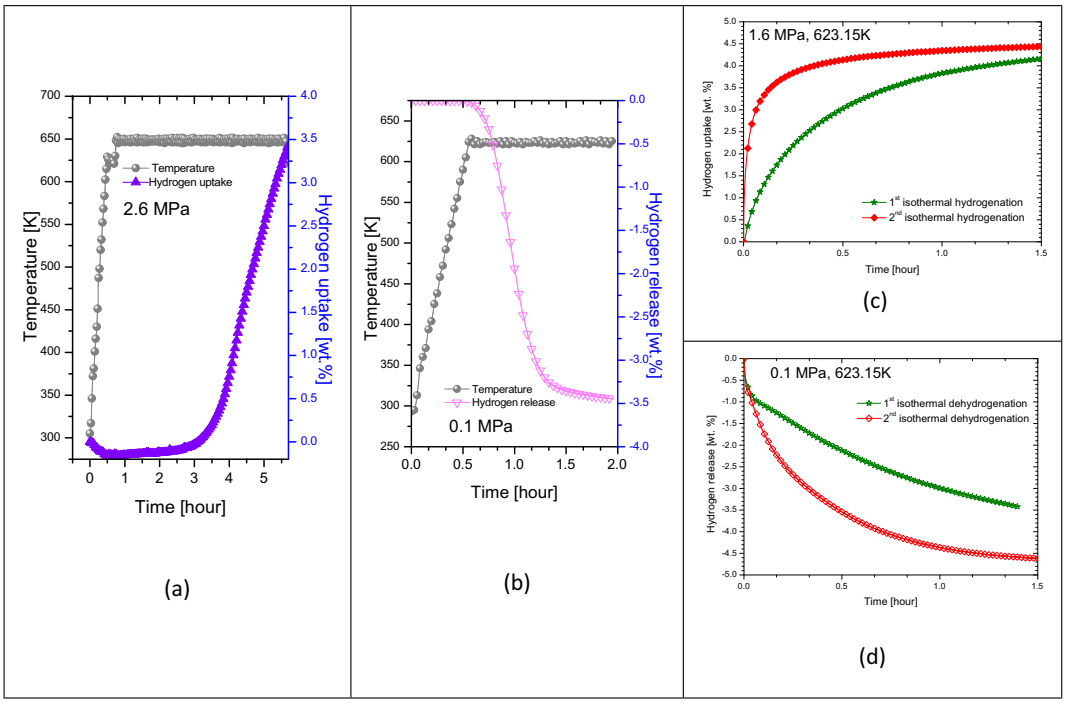

Fig. 8. Hydrogenation reactions at of Mg-Ni-C-nanotubes material. (a) and (b) first cycle with heating ramp. (c) and (d) isothermal experiments.

(Inorganic Crystal Structure Database, Karlsruhe) or COD (Crystallography Open Database) databases were used for phase identification. FT-IR characterization was performed in a Nicolet iS10 of Thermo Fisher Scientific. The studied materials were compacted in KBr pellets. The KBr was purchased from Sigma-Aldrich and dried just before the pellet preparation. About 2.5 mg of each material was dispersed in 50 mg of dry KBr. FT-IR data was collected in Attenuated Total Reflectance (ATR) mode.

7.4.1. $LiAlH_4$

Powders of $LiAlH_4$ were purchased from Sigma Aldrich (95% purity) and used as received. The $LiAlH_4$ was ball milled in a Cryomill (Retsch) for 10 min with liquid-N_2 cooling and 30 Hz of frequency of vibration. The ball to powder ratio was 15:1, zirconium oxide balls were used. The preparation of the sample, and the sealing of milling vial were performed in an argon glove box. Dehydrogenation of cryo-milled $LiAlH_4$ was performed in temperature programmed desorption mode (TPD). After appropriate connection of the sample holder to the apparatus, purging of possible residual air, and argon expansion for volume calibration (steps (a) to (j)), an initial pressure of 0.2 MPa (absolute) was used. Then, the oven temperature was increased from room temperature to 533.16 K at 1 K/min heating rate.

7.4.2. Mg

Chips of Mg were purchased from Sigma-Aldrich (99.98%purity) and used as received. The Mg chips were ball milled in a Cryomill (Retsch) at room temperature for 60 min and 30 Hz of frequency of vibration. The ball to powder ratio was 11:1, zirconium oxide balls were used. 3 wt% of methanol was used as milling agent as reported in a previous work [22]. The preparation of sample, and the sealing of the milling vial were performed in an argon glove box. Hydrogenation of Mg was performed in temperature programmed sorption mode. After appropriate connection of the sample holder to the apparatus, purging of possible residuary air, and argon expansion for volume calibration (steps (a) to (j)), an initial pressure of 2.6 MPa (absolute) was used. Then, the oven temperature was increased from room temperature to 623.15 K at 5 K/min heating rate. Dehydrogenations were performed in dynamic vacuum.

7.4.3. Mg-Ni-C nanotubes

This material was fabricated using Mg powder (Riedel de Haen, 99% purity), Ni (Sigma-Aldrich, 99.8% purity, less than 1 μm), Nb_2O_5 (Sigma-Aldrich, 99.99% purity), and MWNT (Sigma-Aldrich, ≥98% purity). The powders were ball milled in a planetary mill during 1 h at 250 RPM. After proper sample weighing and transfer to the apparatus without oxygen contact, and purging of possible residual air, and argon expansion for volume calibration (steps (a) to (j)), an pre-activation was performed. The pre-activation consisted in the heating up to 350 °C in dynamic vacuum for 3 h, and then cooling down to room temperature. After that, an activation cycle of hydrogenation/dehydrogenation was performed by means of TPS (648.15 K and 2.6 MPa (absolute) and TPD (623.15 K and 0.1 MPa (absolute)). Then the steps (p) to (t) were performed to complete two cycles at 623.15 K, and 1.6 MPa (absolute) bar for hydrogenation, and 0.1 MPa (absolute) for dehydrogenation.

8. Conclusions and perspectives

The results presented for hydrogen uptake/release in different materials demonstrated the feasibility of the construction and good performance of a low-cost apparatus for hydrogen storage studies. The apparatus compile several years of trial-errors, experience and efforts. The combination of the features of double lines (sample and reference) with a $\Delta p = \Delta p_{sample} - \Delta p_{reference}$ approach, resulted in an effective way to eliminate small thermal effects, and the need of a differential pressure transducer, and finally to reduce costs. Further improvements in the apparatus must be performed in the near future. For example, the substitution of manual valves for automatic valves and the implementation of operation, data collection and data management in a single software.

Funding sources

This work was supported by UNAM-DGAPA-PAPPIT [IA100817 Estudio del comportamiento masivo de $NaAlH_4$ como material de almacenamiento de hidrógeno obtenido a partir de Al reciclado]. J.L. Carrillo-Bucio, J.R. Tena-Garcia, E.P. Armenta-Garcia, K. Suárez-Alcántara are thankful for the UNAM-DGAPA-PAPPIT founding.

O. Hernandez-Silva and J.G. Cabañas-Moreno were supported by Project SEP CONACYT [221795].

Conflict of interest

None.

Appendix A. Supplementary data

Supplementary data associated with this article can be found, in the online version, at https://doi.org/10.1016/j.ohx.2018.e00036.

References

[1] D.P. Broom, C.J. Webb, Pitfalls in the characterization of the hydrogen sorption properties of materials, Int. J. Hydrogen Energy 42 (49) (2017) 29320–29343, https://doi.org/10.1016/j.ijhydene.2017.10.028.

[2] D.P. Broom, The accuracy of hydrogen sorption measurements on potential storage materials, Int. J. Hydrogen Energy 32 (18) (2007) 4871–4888, https://doi.org/10.1016/j.ijhydene.2007.07.056.

[3] A. Policicchio, E. Maccallini, G.N. Kalantzopoulos, U. Cataldi, S. Abate, G. Desiderio, R. Giuseppe Agostino, Volumetric apparatus for hydrogen adsorption and diffusion measurements: sources of systematic error and impact of their experimental resolutions, Rev. Sci. Inst. 84 (2013), https://doi.org/10.1063/1.4824485.

[4] A.J. Lachawiec Jr., T.R. DiRaimondo, R.T. Yang, A robust volumetric apparatus and method for measuring high pressure hydrogen storage properties of nanostructured materials, Rev. Sci. Inst. 79 (2008), https://doi.org/10.1063/1.2937820, 063906-12.

[5] www.setaram.com/setaram-products/gas-sorption/pctpro-8, (accessed 15.05.2018).

[6] http://www.quantachrome.com/isorb/isorb.html, (accessed 15.05.2018).

[7] Z. Dehouche, R. Djaozandry, J. Goyette, T.K. Bose, Evaluation techniques of cycling effect on thermodynamic and crystal structure properties of Mg_2Ni alloy, J. Alloys Compd. 288 (1–2) (1999) 269–276, https://doi.org/10.1016/S0925-8388(99), 00085-7.

[8] J.M. Blackman, J.W. Patrick, C.E. Snape, An accurate volumetric differential pressure method for the determination of hydrogen storage capacity at high pressures in carbon materials, Carbon 44 (2006) 918–927, https://doi.org/10.1016/j.carbon.2005.10.032.

[9] J.L. Carrillo-Bucio, J.R. Tena-García, K. Suárez-Alcántara, Dehydrogenation of surface-oxidized mixtures of $2LiBH_4$ + Al/additives (TiF_3 or CeO_2), Inorganics 5 (2017), https://doi.org/10.3390/inorganics5040082, 540083-13.

[10] M. Peschke, Wasserstoffspeicherung in Reaktiven Hydrid-Kompositen Einfluss von fluorbasierten Additiven auf das Sorptionsverhalten des MgB_2-LiH-Systems. Diplomarbeit (undergraduate thesis), GKSS-Forschungszentrum Geesthacht GmbH. Helmut-Schmidt-Universität/Universität der Bundeswehr, Hamburg, 2005, p. 38.

[11] A. Züttel, A. Borgschulte, L. Schlapbach, I. Chorkendorf, S. Suda, in: Hydrogen as a Future Energy Carrier, John Wiley & Sons, Wienheim, Germany, 2008, pp. 71–94.

[12] H. Hemmes, A. Driessen, R. Driessen, Thermodynamic properties of hydrogen at pressures up to 1Mbar and temperatures between 100 and 1000 K, J. Phys. C: Solid State Phys 19 (1986) 3571–3585, https://doi.org/10.1088/0022-3719/19/19/013.

[13] U.K. Deiters, R. Macias-Salinas, Calculation of densities from cubic equations of state: revised, Ind. Eng. Chem. Res. 53 (2014) 2529–2536, https://doi.org/10.1031/ie40386641.

[14] E.W. Lemmon, M.L. Huber, J.W. Leachman, Revised standardized equation for hydrogen gas densities for fuel consumption applications, J. Res. Natl. Inst. Stand. Technol. 113 (2008) 341–350.

[15] ASME Boiler and pressure vessel code, VIII Rules for Construction of Pressure Vessels, Division 1, The American Society of Mechanical Engineers, New York, USA, 2010, p. 19.

[16] V. Rakic, L. Damjanovic, Springer Series in Materials Science vol. 154 (2013) 132–134, DOI: 10.1007/978-3-642-11954-5_4.

[17] J. Block, A.P. Gray, The thermal decomposition of lithium aluminum hydride, Inorg. Chem. 4 (3) (1965) 304–305, https://doi.org/10.1021/ic50025a009.

[18] S.I. Orimo, Y. Nakamori, J.R. Eliseo, A. Züttel, C.M. Jensen, Complex hydrides for hydrogen storage, Chem. Rev. 107 (10) (2007) 4111–4132, https://doi.org/10.1021/cr0501846.

[19] J.R. Ares, K.F. Aguey-Zinsou, M. Porcu, J.M. Sykes, M. Dornheim, T. Klassen, R. Bormann, Thermal and mechanically activated decomposition of $LiAlH_4$, Mater. Res. Bull. 43 (5) (2008) 1263–1275, https://doi.org/10.1016/j.materresbull.2007.05.018.

[20] P. Vajeeston, P. Ravindran, R. Vidya, H. Fjellvåg, A. Kjekshus, Huge-pressure-induced volume collapse in $LiAlH_4$ and its implications to hydrogen storage, Phys. Rev. B 68 (2003), https://doi.org/10.1103/PhysRevB.68.212101, 212101-4.

[21] K. Suárez-Alcántara, A.F. Palacios-Lazcano, T. Funatsu, J.G. Cabañas-Moreno, Mg-M-LiH alloys prepared by mechanical milling and their hydrogen storage characteristics, Int. J. Hydrogen Energy 40 (2015) 17344–17353, https://doi.org/10.1016/j.ijhydene.2015.04.083.

[22] X. Hou, R. Hu, T. Zhang, H. Kou, J. Li, Hydrogenation thermodynamics of melt-spun magnesium rich Mg-Ni nanocrystalline alloys with the addition of multiwalled carbon nanotubes and TiF_3, J. Power Sources 306 (2016) 437–447, https://doi.org/10.1016/j.jpowsour.2015.12.050.